# Capping protein is dispensable for polarized actin network growth and actin-based motility

Majdouline Abou-Ghali, Remy Kusters, Sarah Körber, John Manzi, Jan Faix, C. Sykes, Julie Plastino

Capping protein is dispensable for polarized actin network growth and actin-based motility

Majdouline Abou-Ghali[1,2], Remy Kusters[3], Sarah Körber[4], John Manzi[1,2], Jan Faix[4], Cécile Sykes[1,2], Julie Plastino[1,2,5]

[1] Laboratoire Physico-Chimie Curie, Institut Curie, PSL Research University, CNRS, 75005 Paris, France.
[2] Sorbonne Université, 75005 Paris, France.
[3] Centre de Recherche Interdisciplinaire, Université de Paris INSERM U1284, 75004 Paris, France
[4] Institute for Biophysical Chemistry, Hannover Medical School, 30625 Hannover, Germany
[5] Corresponding author: julie.plastino@curie.fr, +33 156246484

**Running title:** Capping activity can be rendered superfluous

**Keywords**
actin polymerization; actin-based motility; Ena/VASP proteins; capping protein; the Arp2/3 complex; *in vitro* systems

## Abstract

Heterodimeric capping protein (CP) binds the rapidly growing barbed ends of actin filaments and prevents the addition (or loss) of subunits. Capping activity is generally considered to be essential for actin-based motility induced by Arp2/3 complex nucleation. By stopping barbed end growth, CP favors nucleation of daughter filaments at the functionalized surface where the Arp2/3 complex is activated, thus creating polarized network growth, which is necessary for movement. However, here using an *in vitro* assay where Arp2/3 complex-based actin polymerization is induced on bead surfaces in the absence of CP, we produce robust polarized actin growth and motility. This is achieved either by adding the actin polymerase Ena/VASP or by boosting Arp2/3 complex activity at the surface. Another actin polymerase, the formin FMNL2, cannot substitute for CP, showing that polymerase activity alone is not enough to override the need for CP. Interfering with the polymerase activity of Ena/VASP, its surface recruitment or its bundling activity all reduce Ena/VASP's ability to maintain polarized network growth in the absence of CP. Taken together, our findings show that CP is dispensable for polarized actin growth and motility in situations where surface-directed polymerization is favored by whatever means over the growth of barbed ends in the network.

## Introduction

The discovery two decades ago of a mix of purified proteins capable of sustaining actin-based motility in the test-tube was a break-through for understanding how actin dynamics drove movement (1). This system consisted of bacteria propelled forward via the localized polymerization of an actin tail or "comet". Use of variants of this system led, and continue to lead, to major discoveries in the biochemistry of motility and the mechanisms of force production (2-6). The first minimal protein mix consisted of filamentous actin, an actin polymerization nucleator (the Arp2/3 complex) and its activator on the surface of the bacterium, a depolymerization factor (ADF/cofilin) and a capping protein. More recent versions of this system include profilin-actin to more closely mimic *in vivo* conditions of high actin monomer conditions, and often don't include ADF/cofilin, as filament disassembly to replenish monomer levels is not required in the profilin-actin system provided reaction times are kept short (7). However capping activity has been confirmed to be absolutely essential for polarized actin network growth and actin-based motility induced by Arp2/3 complex filament nucleation in many studies (1,4,8-10). The one notable exception is when high amounts of the Arp2/3 complex are present (4). In this case comets indeed form, but motility is inefficient.

These experiments beg the question as to why capping activity is necessary for motility in most cases. Heterodimeric capping protein (CP) tightly binds actin filament barbed ends, stopping their growth. The Arp2/3 complex creates new filaments as branches off the sides of mother filaments, remaining anchored at the pointed end of the daughter filaments, which grow with classical barbed end kinetics in all directions due to random branch orientations (4). The presence of CP in this context results in almost all polymerization occurring via nucleation of new filaments since growing barbed ends are rapidly capped. When nucleation is occurring at a surface due to functionalization to recruit and activate the Arp2/3 complex there, this results in growth predominantly at the surface, and this polarized growth is what produces actin-based motility (4,11). In the absence of CP, filaments are nucleated and grow at the surface, but also grow everywhere else in the network. This gives unpolarized growth that is not able to produce movement. In the one case mentioned above where CP is not necessary for movement, it appears that the excess of Arp2/3 complex present in the reaction boosts nucleation at the surface, providing some actin growth polarity and modest motility (4). It is of note that reconstituted motility based on another actin polymerization nucleator, formin, does not require CP and is in fact inhibited by

it (12). Formin creates new filaments without branching and remains attached to the growing barbed end, where it enhances barbed end elongation in the presence of profilin, and interferes with CP binding (12-15). When formin is immobilized on a surface, formin's mechanism of action means that filament growth is coupled to the surface, actin polymerization is polarized and propulsion occurs without the need for CP, as opposed to motility based on nucleation by the Arp2/3 complex.

Similar to formins Ena/VASP proteins enhance barbed end elongation and impede CP binding to barbed ends, although Ena/VASP proteins are not actin polymerization nucleators in physiological salt conditions (16-18). However the N-terminal EVH1 domain of Ena/VASP proteins is known to bind the proline-rich domain of the Arp2/3 complex activators WASP, WAVE and ActA (19-21), and Ena/VASP proteins are clearly linked to enhanced Arp2/3 complex-based lamellipodial protrusion and motility in cells (20,22-24). Here we sought to understand how barbed end elongators, like Ena/VASP proteins, synergize with the Arp2/3 complex. Employing an *in vitro* system to address this question, we fortuitously observed that the presence of Ena/VASP made CP unnecessary for polarized actin growth and movement, even though actin polymerization nucleation was occurring via the Arp2/3 complex. In fact we found that augmented surface polymerization by any means, including excess Arp2/3 complex as previously reported (4), made CP superfluous. CP is of course present *in vivo* and its contribution to regulating the available pool of actin monomers and controlling Arp2/3 complex-based force production has been established in exquisite detail (7,25) and references therein. Based on this there is a general conception that capping activity is necessary for motility driven by Arp2/3 complex nucleation. We show here that conditions can be found where this is not the case.

## Results and Discussion

### VASP protein can replace CP in a bead motility assay

Our *in vitro* system consisted of profilin-actin, CP, the Arp2/3 complex and 1 μm diameter beads, coated with the pVCA domain of the human WASP protein, an activator of the Arp2/3 complex. We also used the mouse Ena/VASP protein VASP, which increased barbed end elongation by about 35% as measured by TIRF microscopy: at 1.5 μM profilin-actin, elongation speeds were 1.3 ± 0.4 μm/min without VASP and 1.8 ± 0.4 μm/min in the presence of VASP ($p = 0.002$) (Supplementary Figure S1). This is in the same range as the 20% enhancement reported for human VASP under comparable salt conditions, using a similar TIRF method (18) although much smaller than the seven-fold enhancement observed for *Dictyostelium* VASP (17).

As has been observed in numerous previous studies in the presence of CP, actin comets formed on the beads and pushed them forward (Figure 1A and Supplementary Figure S2), while in the absence of CP, no comets were observable, (26) and references therein. Unexpectedly adding VASP to the assay instead of CP produced robust actin comet formation and bead motility (Figure 1A and Supplementary Figure S2). Beads moved at speeds of about 0.68 ± 0.04 μm/min with VASP in the absence CP, and 0.5 ± 0.1 μm/min with CP in the absence of VASP, comparable to what has been observed previously in the reconstituted extract system (20,27). In the past, Ena/VASP proteins in the presence of CP have been studied extensively using bead or bead-type systems, and found to enhance Arp2/3 complex-based bead motility (20,28-30). In these cases Ena/VASP was recruited to the surface, where it exercised its barbed end elongation enhancement activity on freshly-nucleated barbed ends since all other barbed ends were capped by CP. In the absence of CP, VASP would enhance barbed end elongation everywhere in the network, not just at the surface, so it was perplexing as to how VASP

in the absence of CP could rescue polarized actin growth and movement.

**VASP restores polarized actin network growth in the absence of CP**

In order to shed light on how VASP could substitute for CP, we turned to a two-color approach where actin assembly was initiated in one color of actin (labeled with Alexa 594), allowed to polymerize, chased with another color (labeled with Alexa 488) and then observed. This is a classical way to identify where polymerizing ends are located in a network by following the incorporation of the second color (9,10). For these experiments, we used large beads (4.5 µm diameter) to slow down comet formation as the time for comet formation increases with the size of the bead (10). This allowed us to examine actin cloud formation at the bead surface, as clouds never completely polarized to form comets on these beads although some asymmetric clouds were observed. In the presence of CP, the new (green) actin was enriched at the surface, distinct from the older (magenta) actin layer (Figure 1B and Supplementary Figure S3). We called this separation of colors "color segregation", and this indicated polarized actin growth at the bead surface, as occurs in actin-based motility. Adding VASP in the absence of CP gave a similar result (Figure 1B and Supplementary Figure S3). In the absence of CP and VASP, overlap of the two colors was complete (Figure 1B and Supplementary Figure S3), consistent with unpolarized actin growth where uncapped barbed ends in the body of the network were polymerizing, in addition to new branches forming at the surface. We quantified color segregation for a whole population of beads: without CP, only 13% of beads displayed color segregation (N = 90), while CP addition or VASP addition without CP produced segregated colors on 66% (N = 41) and 95% (N = 93) of beads, respectively.

**Increasing Arp2/3 complex activity also restores polarized actin network growth in the absence of CP**

We confirmed previous results by observing that a three-fold increase in Arp2/3 complex concentration could produce color segregation in no CP conditions on 71% of the beads (N = 55, Figure 2A and Supplementary Figure S4). Along the same lines when beads were coated with a tetrameric form of pVCA (S-pVCA) that activated the Arp2/3 complex four-fold more efficiently than GST-pVCA (Supplementary Figure S5), color segregation was observed in the absence of CP, despite normal Arp2/3 complex concentration (50 nM) on 62% of the beads (N = 37, Figure 2A and Supplementary Figure S4). Multimeric forms of WASP, such as S-pVCA, are believed to be more effective for Arp2/3 complex activation due to increased affinity for the Arp2/3 complex (31). All together these results suggested that VASP was somehow enhancing Arp2/3 complex activity since VASP addition gave a similar result to increasing Arp2/3 complex concentration or activation.

**VASP can compensate for sub-optimal concentrations of the Arp2/3 complex in the absence of CP**

To better understand the interplay between VASP and the Arp2/3 complex, we examined network polarity for a range of concentrations of the Arp2/3 complex and VASP in the absence of CP (Figure 2B). At low concentrations of the Arp2/3 complex and VASP, beads displayed weak fluorescence and no color segregation. As described above, at high concentrations of the Arp2/3 complex alone, actin networks around the beads were polarized and colors were segregated. On the other hand, at lower concentrations of the Arp2/3 complex, addition of VASP restored surface-directed polymerization in a dose-dependent manner (Figure 2B). VASP compensation for sub-optimal concentrations of the Arp2/3 complex suggested the possibility that VASP was somehow enhancing Arp2/3 complex activity. In this context, it is of note that there is no known direct interaction between VASP and the Arp2/3 complex (32).

**Effect of VASP on branching in the network**

Increased Arp2/3 complex activity should translate to more branches in the actin network. We evaluated this using fluorescently-labeled

Arp2/3 complex and actin (Figure 2C). We observed that adding VASP in the absence of CP increased the total amount of actin around the beads at about 15 minutes incubation by 2.5-fold as compared to no VASP/+CP conditions. On the other hand, the difference in the total amount of Arp2/3 complex in the network was not significantly different (Figure 2C). This indicated that VASP was not increasing Arp2/3 complex activity and the incidence of branching in the actin network. In fact increased amount of actin and constant amount of the Arp2/3 complex indicated that the network was less branched in the presence of VASP, in keeping with our and others' previous results linking VASP to a reduction in filament branching (23,29,30,33).

**Another form of VASP, but not the elongator FMLN2, can maintain network polarity in the absence of CP**

Having ruled out increased Arp2/3 complex activity to explain our results with VASP, we next wondered whether the ability to substitute for CP was specific to mouse VASP or could be generalized to other barbed end elongators, including other Ena/VASP proteins. In order to test non-mouse Ena/VASP proteins with a range of barbed end elongation enhancement capacities, we turned to human/*Dictyostelium* VASP chimeras, containing a high affinity G-actin-binding site and equipped with different multimerization domains that modulated their activities: the dimer (VASP-2M) increased barbed end elongation by about 50%, the tetramer by 4-fold and the hexamer by 6-fold (34). When applied to beads in the two-color experiment, VASP-2M had a color-segregating effect comparable to mouse VASP (Figure 3A), despite the nucleation activity of this VASP protein, which produced filaments in the bulk thus inhibiting growth on the bead surfaces. Indeed the more active tetrameric and hexameric forms of VASP could not be examined in the two-color experiments as they nucleated drastically, preventing polymerization on the beads.

To test whether elongation enhancement in general could substitute for CP, we next examined the formin FMNL2, known to be a weak nucleator but a good elongator in profilin-actin (35). With a truncated form of FMNL2, FMNL2-8P, containing the profilin-actin recruitment site and the catalytic FH2 domain, we confirmed an enhancement of filament elongation, although FMNL2-8P was less active than VASP (Supplementary Figure S6). When this formin was applied to beads in the absence of CP, color segregation was never observed (Figure 3A). This result indicated that barbed end elongation enhancement alone was not sufficient to overcome the requirement for CP in polarized actin network growth. We also tested the mDia1-FH1-FH2, but this formin nucleated polymerization extensively in the bulk, preventing surface polymerization, as observed with multimeric forms of VASP, mentioned above.

**Restoring polarity with VASP depends partly on its surface recruitment and tetramerization**

VASP's polymerase activity is known to come from cooperation between its F-actin binding domain (FAB) and its G-actin binding domain (GAB), where FAB targets VASP to barbed ends and GAB contributes its bound monomer to filament growth (17,18,34,36-38). In keeping with this, deleting VASP's FAB domain reduced color segregation to such an extent as to not be significantly different from adding nothing at all (23%, N = 69, Table 1). Surprisingly mutating VASP's GAB domain had no effect on color segregation (88%, N = 86, Table 1). However deleting the polyproline (PP) domain, which binds profilin-actin, significantly reduced color segregation (78%, N = 68, Table 1). In our profilin-actin system, it seemed that PP played the major role for VASP polymerase activity.

VASP is recruited to pVCA-coated beads, via the interaction between VASP's EVH1 domain and the proline-rich domain of pVCA (20). To test the possibility that VASP was exercising its effect via surface recruitment, we deleted the EVH1 domain of VASP. This mutant displayed significantly less color segregation than the wild-type (73%, N = 82, Table 1).

Although diminished, the fact that there was considerable polarity maintenance in the presence of ΔEVH1-VASP suggested that there were compensatory mechanisms at play. Another mechanism for surface bias could stem from a preference of VASP for freshly polymerized ATP-actin, but it is known that VASP binding to actin is independent of its nucleotide state (18,28).

It is known that VASP is able to bundle filaments via its tetramerization domain (TET) (39,40). Bundling could hold filaments in an orientation more favorable for assembly towards the surface, an effect that would not be relevant for filaments growing in the bulk network. To test this idea, we deleted the TET domain and observed that indeed color segregation was significantly reduced compared to wild-type (78%, N = 117, Table 1). Since oligomerization also contributes to barbed end elongation enhancement activity, we could not rule out that this reduction was due to an effect on polymerase activity, but in conditions such as ours, where VASP molecules were clustered on a surface, TET would no longer be needed for optimal polymerase activity (17). Unfortunately it wasn't possible to observe the fine structure of actin filaments by transmission electron microscopy on bead surfaces due to the thickness of the sample, so we couldn't confirm changes in surface organization of filaments in the presence of VASP. However we know from previous studies that VASP has the effect of aligning filaments in the direction of movement in actin comets (29). That said ablating the bundling activity of VASP had only a minor effect on color segregation, and thus could not be the whole explanation. Indeed previous studies gave no indication that bundling proteins such as fascin and α-actinin could stand in for CP in actin-based motility (41).

In summary for the VASP mutants, removal of the F-actin binding site drastically reduced color segregation, while altering the G-actin binding site had no effect at all. Deleting the other functional domains (profilin-actin binding, tetramerization and surface recruitment) significantly reduced color segregation, but nevertheless these deletions were able to support considerable network polarity. Overall these results indicated that there were potentially multiple ways for VASP to favor surface polymerization, enabling the polymerization of uncapped barbed ends at the bead surface to outstrip uncapped barbed end polymerization in the network, thus giving polarized actin network growth on large beads and actin-based motility on small beads.

**Temporal evolution of network growth in the absence of CP**

We developed a model of how actin polymerizes at a surface over time to evaluate the effect of removing CP. In our bead system, the formation of new filaments occurred exclusively at the bead surface for two main reasons. First the Arp2/3 complex is an inefficient nucleator unless activated by pVCA, which was present only on the bead surface. Second we used profilin-actin, which curbed the spontaneous nucleation of filaments away from the bead surface (7). Since the Arp2/3 complex nucleates new filaments as branches off the sides of existing mother filaments, the source term for new polymerizing filaments is therefore branch formation.

The growth of the actin network around the bead can then be described with three kinetic rates: $v_b$, the branching rate, $v_p$, the barbed end elongation rate of filaments, and $v_c$, the capping rate that terminates filament elongation. All of this can be combined into a simple growth model, expressing the temporal evolution of the total amount of actin in the network around a single bead, expressed as a volume, $V$. $V$ is a function of the number of polymerizing ends, $N_{act}$ , $v_p$ and $a^3$, the volume added to a growing filament with the addition of each monomer (Eq. 1).

$$\frac{dV}{dt} = v_p a^3 N_{act} \quad (1)$$

$N_{act}$ in turn varies over time inversely to the capping rate and proportionally to the source term, $v_b n_s$, which is the number of activators

(pVCA molecules) on a bead surface, $n_s$, multiplied by the branching rate (Eq. 2).

$$\frac{dN_{act}}{dt} = -v_c N_{act} + v_b n_s \quad (2)$$

Integrating Eq. 2 and assuming that at time 0, $N_{act} = 0$ gives an expression for $N_{act}$ (Eq. 3).

$$N_{act} = \frac{v_b n_s}{v_c}(1 - e^{-v_c t}) \quad (3)$$

Plugging this expression for $N_{act}$ into Eq. 1 and solving for $V(t)$ gives Eq. 4.

$$V(t)_{+CP} = \frac{v_p v_b n_s}{v_c^2}(e^{-v_c t} + (v_c t - 1))a^3 \quad (4)$$

In the absence of capping ($v_c$ = 0) in Eq. 2, $N_{act}$ equals $v_b n_s t$ and $V(t)_{no\ CP}$ can then be expressed by Eq. 5.

$$V(t)_{no\ CP} = \frac{v_p v_b n_s}{2} t^2 a^3 \quad (5)$$

Equations 4 and 5 describe the amount of actin that forms on the bead surface as a function of time in the presence and absence of CP, respectively. From comparing these equations, we can see that the amount of actin is very highly impacted by the presence of capping ($v_c^2$ term in the denominator of Eq. 4), and that the amount of actin grows quadratically with time in the absence of CP ($t^2$ in Eq. 5), while approximately linearly with time in the presence of capping since the term $e^{-v_c t}$ is small.

To get an idea of order of magnitudes, taking literature values for $v_c$ and $a^3$ and our estimated or measured values for $v_b$, $v_p$, $v_p^{+VASP}$ and $n_s$ (see Experimental Procedures), we calculated that at 2 minutes reaction time, +VASP/no CP beads should already have 6-fold more actin around them than +CP beads. Most of this effect derives from the absence of CP not the increased elongation in the presence of VASP.

We compared this estimate to experimental data. We measured actin accumulation over time and observed that at 2 minutes, there was a 3-fold difference between +VASP/no CP and +CP conditions (Figure 3B), and even at longer incubation times and also as observed in Figure 2C, +VASP/no CP did not increase quadratically as predicted. The discrepancy between model and experiments concerning quantification of total actin around beads over time in the absence of CP is probably due to several factors. First the model probably over-estimates actin assembly rates as it doesn't take into account local monomer depletion effects, shown to be important even in conditions of high monomeric actin in the bulk (6). Second the experimental measurement probably under-estimates the amount of actin around the beads. A growing actin layer on a bead has a far-reaching actin cloud that is 10 times bigger than the part that is visible by fluorescence microscopy, and reduced CP conditions makes this effect even more pronounced (42). Although the differences in actin accumulation that we observed in the presence of CP versus in no CP/+VASP conditions were of the right order of magnitude as compared to the model, the main conclusion from this analysis was that VASP's modest barbed end elongation enhancement activity had a relatively minor effect on actin growth, overshadowed by the presence/absence of CP.

The novel role of VASP that we reveal in this study is its ability to render CP unnecessary for motility and polarized actin network growth on beads. VASP appears to achieve this by selectively promoting surface assembly in the presence of Arp2/3 complex nucleation via a combination of barbed end elongation enhancement, surface recruitment and actin filament bundling. This bias is enough to drastically change outcome and allow polarized actin network growth and motility in the absence of CP. Likewise we show that other conditions that increase surface polymerization rescue polarity, indicating that CP is not an absolute requirement for Arp2/3 complex-based polarized actin growth and motility.

## Experimental Procedures

### DNA and proteins

Rabbit muscle actin, pyrene-labeled rabbit muscle actin and porcine Arp2/3 complex were

purchased from Cytoskeleton as lyophilized powder and resuspended as per the manufacturer's instructions. Fluorescently-labeled (Alexa 488 and Alexa 594) rabbit muscle actin was purchased from Invitrogen. All other proteins were purified or labeled in-house. The Arp2/3 complex was fluorescently labeled by incubation with a 10-fold molar excess of Alexa 488 C5-maleimide on ice for 3 hours. 1 mM DTT was added to quench the labeling and the protein was dialyzed overnight in 20 mM Tris, pH 7.4, 25 mM KCl, 0.25 mM DTT, 100 µM ATP, 1 mM MgCl2, 0.5 mM EDTA, centrifuged to remove precipitate and frozen. The DNA constructs for untagged human profilin and GST-pVCA-WASP-His (human WASP, residues 150-502, equipped with a GST and a 8-histidine tag, called GST-pVCA) were gifts of T. Pollard (Yale University) and L. Blanchoin (CEA Grenoble), respectively. Profilin was purified as in (43) and GST-pVCA as in (20). The streptavidin tagged pVCA-WASP-His construct (S-pVCA) was purified as in (43).

The DNA constructs for mouse α1β2 CP and wild-type and mutant forms of mouse VASP were gifts from D. Schafer (University of Virginia), and the proteins were purified as in (44) for CP and as in (16) for VASP and VASP mutants. VASP proteins were further purified via FPLC using a Superdex 200 10/300GL column (GE Healthcare). VASP mutants were ΔEVH1-VASP, lacking residues 1–114; ΔGAB-VASP, carrying the double point mutation R232E, K233E in the G-actin binding site; ΔPP-VASP, lacking residues 156–207; ΔFAB-VASP, lacking residues 255–273; and ΔTET-VASP, lacking residues 331–375. mVASP concentrations were calculated with the tetramer molecular weight. The chimera VASP-2M was purified as in (34) and its concentration is represented in monomers. mDia1-FH1-FH2 was purified as in (45).

The GST-FMNL2-8P construct was the kind gift of J. Pernier (I2BC, Paris-Saclay) [21]. The construct was transformed into Rosetta 2(DE3) pLysS E.coli cells (Novagen), and grown in 2 L of 2YT medium with antibiotics. Expression was induced with 1 mM IPTG, 20ºC, overnight. Cells were lysed by sonication in Lysis Buffer: 20 mM Tris pH 7.5, 500 mM NaCl, 1 mM EDTA and 1 mM DTT, supplemented with 1 mM PMSF and complete EDTA-free protease inhibitor cocktail (Roche). Protein was bound to Glutathione Sepharose 4 fast flow beads (GE Healthcare). Unbound proteins were washed away with Lysis buffer, and bound proteins eluted in 20 mM Tris pH7.5, 150 mM NaCl, 1 mM DTT, 25 mM Reduced Glutatione pH 7.5. For GST tag removal, a final of 1 mM EDTA was added to samples, plus 50 µg of PreScission Protease. GST was cleaved overnight at 4º C. The sample was further purified in Buffer 20 mM Tris pH7.5, 50 mM KCl, 1 mM DTT, using the HiLoad Superdex 200 16/600 pg column. The peak containing FMNL2 was collected, frozen in liquid nitrogen and stored at -80°C.

All protein concentrations were measured by Bradford assay.

**Bead preparation**

For bead assays carboxylate beads (Polysciences) were used. 9 µL of 2.5 % bead suspension, 4.5 µm diameter, or 2 µL of 2.5 % bead suspension, 1.0 µm diameter (total surface area 3 $cm^2$) were coated in 40 µL of 2 µM GST-pVCA-WASP or S-pVCA-WASP in Xb (10 mM HEPES pH 7.5, 0.1 M KCl, 1 mM $MgCl_2$, and 0.1 mM $CaCl_2$). The reaction was mixed in a thermomixer for 20 minutes at 18°C and 1000 rpm. After coating, the bead surface was blocked by washing twice with 1% BSA (Bovine Serum Albumin)/Xb buffer. The coated beads were resuspended in 120 µL Xb/1% BSA and stored on ice for a day of experiments.

**Actin polymerization on beads**

Actin was thawed, diluted to approximately 20-30 µM in G-buffer (2 mM Tris, 0.2 mM $CaCl_2$, 0.2 mM DTT, 0.2mM ATP pH 8.0) and allowed to depolymerize at 4°C for at least 2 days and then kept on ice and used for several weeks. Profilin, CP, the Arp2/3 complex, and KCl were all diluted in MB13 buffer (10 mM HEPES, 1.5 mM ATP, 3 mM DTT, 1.5 mM

$MgCl_2$, 1 mM EGTA, 50 mM KCl, 1% BSA, pH 7.5). VASP proteins were diluted in VASP buffer (20 mM Imidazole, 200 mM KCl, 1 mM EGTA, 2 mM $MgCl_2$, 1 mM DTT, pH 7.0).

The *in vitro* actin polymerization reaction mix contained: 0.2 µL of coated beads (approximately 0.005 $cm^2$ of surface), 50 nM Arp2/3 complex, 5 or 15 µM profilin (either a 1:1 ratio or a 1:3 ratio) and 5 µM G-actin, with or without 25 nM CP and/or 50 nM VASP, except for the phase diagram experiments where the concentrations of the Arp2/3 complex and VASP were varied, and the spinning disc experiments that were performed at 37 nM VASP. The final KCl concentration was adjusted to 86 mM by addition of KCl in MB13. The final reaction volume was 8.4 µL. The entire reaction was spotted on a glass slide, covered with a coverslip (18 × 18 mm) and sealed with vaseline/lanolin/paraffin (VALAP) (1:1:1). For timed experiments, the stopwatch was started upon addition of actin, which was always added last.

**Two-color experiments**

Reaction conditions were as described above, but with Alexa 488 or Alexa 594-labeled actin added to the diluted unlabeled actin solution in G-buffer to a final concentration of 10 % labeled actin, and allowed to depolymerize before use. For the two-color experiment, a half-batch (4.1 µL) of actin polymerization reaction mix + beads (see above) was prepared with Alexa 594-labeled actin and was allowed to polymerize in the tube at room temperature until actin polymerization was well underway (anywhere from 5-20 minutes depending on conditions). This reaction was then mixed with a second reaction mix (8.4 µL) containing Alexa 488-labeled actin, but no beads. The entire mixture was spotted on a slide and photographed over time, with the best color segregation observed at 10-20 minutes reaction time (images shown in the main figures), although clouds continued to grow for several hours.

**Bead observation and data processing**

Phase contrast and epifluorescence microscopy images were obtained on an Olympus IX70 inverted microscope with a 100x oil-immersion objective and CoolSnap CCD camera (Photometrics). Spinning disc images were obtained on an inverted confocal spinning disk microscope from Nikon using a 100x oil objective and a CoolSNAP HQ2 camera (Photometrics). Phase contrast and fluorescence quantification was done using MetaMorph software (Universal Imaging). For speed estimations, pictures of 1 µm beads with comets were taken randomly over the whole slide for about 20 minutes, lengths were plotted versus time, and the slopes were taken as the average speed. For two-color experiments, pictures of beads were taken randomly over the whole slide. For each bead, 2 pictures were taken, one for green fluorescence and one for red fluorescence, and the two pictures were overlaid in MetaMorph. The linescan function of MetaMorph was used on the combined images, drawing a line from the center of the bead towards the outside. This gave the intensity of each pixel in the red and green channel with respect to its position along the line, and was plotted after subtracting the background, taken at the furthest extreme of the linescan from the bead surface. Linescans were drawn by hand at a location that gave the best color segregation profile regardless of conditions.

For Arp2/3 complex quantification coupled with actin measurements, bead stacks were imaged by spinning disc at approximately 10-20 minute reaction time, where growth had plateaued. A single plane where the bead appeared largest was taken, and densities were evaluated in Metamorph by drawing a doughnut shape that surrounded the bead and included 1 µm of the network around the bead. Background was subtracted. For temporal evaluation of actin growth, bead stacks were taken over time by spinning disc, and the maximum intensity projection of the two central planes (where the bead appeared the largest) was analyzed using a Matlab script to measure the total fluorescence intensity in the

entire image (one bead per field). For all data significant differences were calculated and p values reported using the Student t-test for comparison of averages, and a Chi-squared test for comparison of %. $p < 0.05$ was taken as significant.

**Actin polymerization assessment by pyrene assay**

For assessment of GST-pVCA and S-pVCA activity, the pyrene assay mix (60 µL final volume) contained 50 nM Arp2/3 complex, 15 µM profilin, 5 µM actin (~5% labeled with pyrene, diluted to 30 µM in G-buffer and allowed to depolymerize for at least 2 days before use) and 86 mM KCl in MB13 buffer. GST-pVCA and S-pVCA were diluted in MB13. For assessment of FMNL2-8P activity, the same mix was used, minus the Arp2/3 complex. Seeds were formed by allowing actin to polymerize to a plateau in the absence of profilin, and then kept on ice. Approximately 0.4 µM of actin filaments was used to seed each reaction. For all curves, as soon as monomeric actin was added, the mix was placed in a glass cuvette and the fluorescence intensity (excitation 365 nm, emission 407 nm, excitation slit 5 nm, emission slit 5 nm) was measured every second using a fluorimeter (Cary) thermostatted at 20°C. Kaleidagraph was used to plot the data. The concentration of barbed ends was calculated with the equation: [b.e.] = (elongation rate $\mu Ms^{-1}$)/($k_+$[actin monomers]), where elongation rate at half-maximum was converted from a.u. to µM based on the curve plateau assuming all actin was in filamentous form at this point, using 2.5 µM as the actin monomer concentration at half-max and taking $k_+$ as approximately 10 $\mu M^{-1}s^{-1}$ (46,47).

**Single filament assay by TIRF microscopy**

Glass coverslips were cleaned in a glass holder using 1M NaOH and sonication for 15 minutes, then washed in water, sonicated again in ethanol 96% for 15 minutes, washed in water and dried using pressure nitrogen flow. Clean coverslips were assembled into chambers where the sample was sandwiched between an 18 x 18 mm and a 24 x 50 mm coverslip separated by double-sided tape. Experiments were performed using an Eclipse Ti Inverted Microscope with a 100x oil immersion objective and a Quantum 512SC camera (Photometrics). Actin polymerization mix contained 1.5 µM of Alexa-488 labeled actin (15% labeling), 1.5 µM profilin, 86mM KCl, 0.2% DABCO and 4% methylcellulose in MB13. VASP was added at 37 nM. Samples were flowed into the chambers and sealed with VALAP. Image acquisition started 1 minute after the start of polymerization in the chamber. Images were collected at 1 second interval for 15 minutes. Actin filament lengths were measured over time, and converted to rate constants by considering that 1 µm represented 370 subunits of actin (48). At least 16 filaments were measured for each condition.

**Constants used in the calculations**

The rate of capping, $v_c$ , was taken as 0.065 $s^{-1}$, based on our CP concentration of 25 nM and the rate constant of $2.6 \times 10^6$ $M^{-1}s^{-1}$ (49). The volume added per monomer addition event, $a^3$, was $(2.7\ nm)^3$ (48). The number of activators on a bead surface, $n_s$, was calculated as $2.5 \times 10^6$ from the pVCA spacing of 5 nm (50) and the surface area of a 4.5 µm diameter bead. The polymerization rate, $v_p$, was calculated as 28 $s^{-1}$ in the absence of VASP and 37 $s^{-1}$ in the presence of VASP, $v_p^{+VASP}$. These values derive from the monomeric actin concentration in our assay of 5 µM and our measured barbed end $k_+$of around 5.5 $\mu M^{-1}s^{-1}$ in the absence of VASP and 7.4 $\mu M^{-1}s^{-1}$ in the presence of VASP, measured by TIRF microscopy. 5.5 $\mu M^{-1}s^{-1}$ is half the value observed without profilin (about 10 $\mu M^{-1}s^{-1}$ (47)), due to the inhibitory effect of excess or stoichiometric profilin on barbed end polymerization (18,51). The branching rate, $v_b$, was estimated from the known mesh size of about 50 nm (50) and the dependency of mesh size on polymerization, monomer size and branching: $\xi = av_p/v_b$, giving $v_b$ as 1.5 $s^{-1}$. This value of $v_b$ was used for +VASP conditions as well, as there are indications that mesh size is larger in the presence of VASP (23,29) thus potentially compensating for increased $v_p$.

**Data availability statement**
All data associated with this paper are included in the manuscript and in the supplementary information.

**Acknowledgments**
We warmly acknowledge Olivier Renaud et Olivier Leroy of the Cell and Tissue Imaging Platform (member of France BioImaging, ANR-10-INBS-04) of the Genetics and Developmental Biology Department (UMR3215/U934) of Institut Curie for help with light microscopy.

**Funding information**
J.P. acknowledges financial support for this work from the Fondation pour la Recherche Médicale (Grant DEQ20120323737) and the Fondation ARC (Grant PJA 20151203487 and Grant PJA 20191209604). This work also received support under the program "Investissements d'Avenir" launched by the French Government and implemented by ANR (ANR-10-LABX-0038 and ANR-10-IDEX-0001-02 PSL), including post-PhD financing of M. A.-G. M. A.-G. was funded by a PhD fellowship from La Ligue Contre le Cancer. S.K. was supported by the ERASMUS+ Student Mobility Placement program. R.K. thanks the Bettencourt Schueller Foundation long term partnership, and was partly supported by CRI Research Fellowship program.

**Declaration of Interests**
The authors declare that they have no conflicts of interest with the contents of this article.

## References


1. Loisel, T. P., Boujemaa, R., Pantaloni, D., and Carlier, M. F. (1999) Reconstitution of actin-based motility of Listeria and Shigella using pure proteins. *Nature* **401**, 613-616
2. Cameron, L. A., Footer, M. J., Van Oudenaarden, A., and Theriot, J. A. (1999) Motility of ActA protein-coated microspheres driven by actin polymerization. *Proceedings of the National Academy of Sciences* **96**, 4908-4913
3. Bernheim-Groswasser, A., Wiesner, S., Golsteyn, R. M., Carlier, M.-F., and Sykes, C. (2002) The dynamics of actin-based motility depend on surface parameters. *Nature* **417**, 308-311
4. Achard, V., Martiel, J.-L., Michelot, A., Guérin, C., Reymann, A.-C., Blanchoin, L., and Boujemaa-Paterski, R. (2010) A "Primer"-Based Mechanism Underlies Branched Actin Filament Network Formation and Motility. *Curr. Biol.* **20**, 423-428
5. Reymann, A.-C., Boujemaa-Paterski, R., Martiel, J.-L., Guérin, C., Cao, W., Chin, H. F., De La Cruz, E. M., Théry, M., and Blanchoin, L. (2012) Actin network architecture can determine myosin motor activity. *Science* **336**, 1310-1314
6. Boujemaa-Paterski, R., Suarez, C., Klar, T., Zhu, J., Guérin, C., Mogilner, A., Théry, M., and Blanchoin, L. (2017) Network heterogeneity regulates steering in actin-based motility. *Nat. Commun.* **8**, 655
7. Plastino, J., and Blanchoin, L. (2019) Dynamic stability of the actin ecosystem. *J. Cell Sci.* **132**, jcs219832
8. Dürre, K., Keber, F. C., Bleicher, P., Brauns, F., Cyron, C. J., Faix, J., and Bausch, A. R. (2018) Capping protein-controlled actin polymerization shapes lipid membranes. *Nat. Commun.* **9**, 1630
9. Akin, O., and Mullins, R. D. (2008) Capping protein increases the rate of actin-based motility by promoting filament nucleation by the Arp2/3 complex. *Cell* **133**, 841-851
10. van der Gucht, J., Paluch, E., Plastino, J., and Sykes, C. (2005) Stress release drives symmetry breaking for actin-based movement. *Proc. Natl. Acad. Sci. U.S.A.* **102**, 7847-7852
11. Sykes, C., and Plastino, J. (2010) Actin filaments up against a wall. *Nature* **464**, 365-366
12. Romero, S., Le Clainche, C., Didry, D., Egile, C., Pantaloni, D., and Carlier, M.-F. (2004) Formin is a processive motor that requires profilin to accelerate actin assembly and associated ATP hydrolysis. *Cell* **119**, 419-429
13. Kovar, D. R., Harris, E. S., Mahaffy, R., Higgs, H. N., and Pollard, T. D. (2006) Control of the assembly of ATP- and ADP-actin by formins and profilin. *Cell* **124**, 423-435
14. Kovar, D. R., Kuhn, J. R., Tichy, A. L., and Pollard, T. D. (2003) The fission yeast cytokinesis formin Cdc12p is a barbed end actin filament capping protein gated by profilin. *J. Cell Biol.* **161**, 875-887
15. Kovar, D. R., and Pollard, T. D. (2004) Insertional assembly of actin filament barbed ends in association with formins produces piconewton forces. *Proceedings of the National Academy of Sciences* **101**, 14725-14730
16. Barzik, M., Kotova, T. I., Higgs, H. N., Hazelwood, L., Hanein, D., Gertler, F. B., and Schafer, D. A. (2005) Ena/VASP Proteins Enhance Actin Polymerization in the Presence of Barbed End Capping Proteins. *J. Biol. Chem.* **280**, 28653-28662
17. Breitsprecher, D., Kiesewetter, A. K., Linkner, J., Urbanke, C., Resch, G. P., Small, J. V., and Faix, J. (2008) Clustering of VASP actively drives processive, WH2 domain-mediated actin filament elongation. *EMBO J.* **27**, 2943-2954
18. Hansen, S. D., and Mullins, R. D. (2010) VASP is a processive actin polymerase that requires monomeric actin for barbed end association. *J. Cell Biol.* **191**, 571-584
19. Castellano, F., Le Clainche, C., Patin, D., Carlier, M.-F., and Chavrier, P. (2001) A WASP-VASP complex regulates actin polymerization at the plasma membrane. *EMBO J.* **20**, 5603-5614

20. Havrylenko, S., Noguera, P., Abou-Ghali, M., Manzi, J., Faqir, F., Lamora, A., Guérin, C., Blanchoin, L., and Plastino, J. (2015) WAVE binds Ena/VASP for enhanced Arp2/3 complex-based actin assembly. *Mol. Biol. Cell* **26**, 55-65
21. Chakraborty, T., Ebel, F., Domann, E., Niebuhr, K., Gerstel, B., Pistor, S., Temm-Grove, C. J., Jockusch, B. M., Reinhard, M., Walter, U., and Wehland, J. (1995) A focal adhesion factor directly linking intracellularly motile Listeria monocytogenes and Listeria ivanovii to the actin-based cytoskeleton of mammalian cells. *EMBO J.* **14**, 1314-1321
22. Rottner, K., Behrendt, B., Small, J. V., and Wehland, J. (1999) VASP dynamics during lamellipodia protrusion. *Nat. Cell Biol.* **1**, 321-322
23. Bear, J. E., Svitkina, T. M., Krause, M., Schafer, D. A., Loureiro, J. J., Strasser, G. A., Maly, I. V., Chaga, O. Y., Cooper, J. A., Borisy, G. G., and Gertler, F. B. (2002) Antagonism between Ena/VASP proteins and actin filament capping regulates fibroblast motility. *Cell* **109**, 509-521
24. Damiano-Guercio, J., Kurzawa, L., Mueller, J., Dimchev, G., Schaks, M., Nemethova, M., Pokrant, T., Brühmann, S., Linkner, J., Blanchoin, L., Sixt, M., Rottner, K., and Faix, J. (2020) Loss of Ena/VASP interferes with lamellipodium architecture, motility and integrin-dependent adhesion. *eLife* **9**, e55351
25. Carlier, M.-F., Pernier, J., Montaville, P., Shekhar, S., and Kühn, S. (2015) Control of polarized assembly of actin filaments in cell motility. Cell Mol Life Sci. 2015;72. *Cell. Mol. Life Sci.* **72**, 3051-3067
26. Caceres, R., Abou-Ghali, M., and Plastino, J. (2015) Reconstituting the actin cytoskeleton at or near surfaces *in vitro*. *Biochem. Biophys. Acta* **1853**, 3006-3014
27. Reymann, A.-C., Suarez, C., Guérin, C., Martiel, J.-L., Staiger, C. J., Blanchoin, L., and Boujemaa-Paterski, R. (2011) Turnover of branched actin filament networks by stochastic fragmentation with ADF/cofilin. *Mol. Biol. Cell* **22**, 2541-2550
28. Laurent, V., Loisel, T. P., Harbeck, B., Wehman, A., Gröbe, L., Jockusch, B. M., Wehland, J., Gertler, F. B., and Carlier, M.-F. (1999) Role of proteins of the Ena-VASP family in actin-based motility of Listeria monocytogenes. *J. Cell Biol.* **144**, 1245-1258
29. Plastino, J., Olivier, S., and Sykes, C. (2004) Actin filaments align into hollow comets for rapid VASP-mediated propulsion. *Curr. Biol.* **14**, 1766-1771
30. Samarin, S., Romero, S., Kocks, C., Didry, D., Pantaloni, D., and Carlier, M.-F. (2003) How VASP enhances actin-based motility. *J. Cell Biol.* **163**, 131-142
31. Padrick, S. B., Cheng, H.-C., Ismail, A. M., Panchal, S. C., Doolittle, L. K., Kim, S., Skehan, B. M., Umetani, J., Brautigam, C. A., Leong, J. M., and Rosen, M. K. (2008) Hierarchical regulation of WASP/WAVE proteins. *Mol. Cell* **32**, 426-438
32. Boujemaa-Paterski, R., Gouin, E., Hansen, G., Samarin, S., Le Clainche, C., Didry, D., Dehoux, P., Cossart, P., Kocks, C., Carlier, M.-F., and Pantaloni, D. (2001) *Listeria* protein ActA mimics WASP family proteins: it activates filament barbed end branching by Arp2/3 complex. *Biochemistry* **40**, 11390-11404
33. Skoble, J., Auerbuch, V., Goley, E. D., Welch, M. D., and Portnoy, D. A. (2001) Pivotal role of VASP in Arp2/3 complex-mediated actin nucleation, actin branch-formation, and *Listeria monocytogenes* motility. *J. Cell Biol.* **155**, 89-100
34. Brühmann, S., Ushakov, D. S., Winterhoff, M., Dickinson, R. B., Curth, U., and Faix, J. (2017) Distinct VASP tetramers synergize in the processive elongation of individual actin filaments from clustered arrays. *Proc. Natl. Acad. Sci. U.S.A.* **114**, E5815-E5824
35. Block, J., Breitsprecher, D., Kühn, S., Winterhoff, M., Kage, F., Geffers, R., Duwe, P., Rohn, J. L., Baum, B., Brakebusch, C., Geyer, M., Stradal, T. E. B., Faix, J., and Rottner, K. (2012) FMNL2 drives actin-based protrusion and migration downstream of Cdc42. *Curr. Biol.* **22**, 1005-1012

36. Breitsprecher, D., Kiesewetter, A. K., Linkner, J., Vinzenz, M., Stradal, T., Small, J. V., Curth, U., Dickinson, R. B., and Faix, J. (2011) Molecular mechanism of Ena/VASP-mediated actin-filament elongation. *EMBO J.* **30**, 456-467
37. Ferron, F., Rebowski, G., Lee, S. H., and Dominguez, R. (2007) Structural basis for the recruitment of profilin-actin complexes during filament elongation by Ena/VASP. *Embo J* **26**, 4597-4606
38. Winkleman, J. D., Bilancia, C. G., Peifer, M., and Kovar, D. R. (2014) Ena/VASP Enabled is a highly processive actin polymerase tailored to self-assemble parallel-bundled F-actin networks with Fascin. *Proc. Natl. Acad. Sci. U.S.A.* **111**, 4121–4126
39. Bachmann, C., Fischer, L., Walter, U., and Reinhard, M. (1999) The EVH2 domain of the vasodilator-stimulated phosphoprotein mediates tetramerization, F-actin binding and actin bundle formation. *J. Biol. Chem.* **274**, 23549-23557
40. Gentry, B., van der Meulen, S., Noguera, P., Alonso-Latorre, B., Plastino, J., and Koenderink, G. (2012) Multiple actin binding domains of Ena/VASP proteins determine actin network stiffening. *Eur. Biophys. J.* **41**, 979-990
41. Vignjevic, D., Yarar, D., Welch, M. D., Peloquin, J., Svitkina, T., and Borisy, G. G. (2003) Formation of filopodia-like bundles in vitro from a dendritic network. *J. Cell Biol.* **160**, 951-962
42. Bussonier, M., Carvalho, K., Lemière, J., Joanny, J.-F., Sykes, C., and Betz, T. (2014) Mechanical detection of a long-range actin network emanating from a biomimetic cortex. *Biophys. J.* **107**, 854-862
43. Carvalho, K., Lemière, J., Faqir, F., Manzi, J., Blanchoin, L., Plastino, J., Betz, T., and Sykes, C. (2013) Actin polymerization or myosin contraction: two ways to build up cortical tension for symmetry breaking. *Phil. Trans. R. Soc. B* **368**, 20130005
44. Palmgren, S., Ojala, P. J., Wear, M. A., Cooper, J. A., and Lappalainen, P. (2001) Interactions with $PIP_2$, ADP-actin monomers, and capping protein regulate the activity and localization of yeast twinfilin. *J. Cell Biol.* **155**, 251-260
45. Rückerl, F., Lenz, M., Betz, T., Manzi, J., Martiel, J.-L., Safouane, M., Paterski-Boujemaa, R., Blanchoin, L., and Sykes, C. (2017) Adaptive response of actin bundles under mechanical stress. *Biophys. J.* **113**, 1072-1079
46. Higgs, H. N., Blanchoin, L., and Pollard, T. D. (1999) Influence of the C terminus of Wiskott-Aldrich syndrome protein (WASp) and the Arp2/3 complex on actin polymerization. *Biochemistry* **38**, 15212-15222
47. Pollard, T. D. (1986) Rate constants for the reactions of ATP- and ADP-actin with the ends of actin filaments. *J. Cell Biol.* **103**, 2747-2754
48. Huxley, H. E., and Brown, W. (1967) The low-angle X-ray diagram of vertebrate striated muscle and its behaviour during contraction and rigor. *J. Mol. Biol.* **30**, 383-434
49. Kuhn, J. R., and Pollard, T. D. (2007) Single molecule kinetic analysis of actin filament capping. *J. Biol. Chem.* **282**, 28014-28024
50. Kawska, A., Carvalho, K., Manzi, J., Boujemaa-Paterski, R., Blanchoin, L., Martiel, J.-L., and Sykes, C. (2012) How actin network dynamics control the onset of actin-based motility. *Proc. Natl. Acad. Sci. U.S.A.* **109**, 14440–14445
51. Pasic, L., Kotova, T., and Schafer, D. A. (2008) Ena/VASP Proteins Capture Actin Filament Barbed Ends. *J. Biol. Chem.* **283**, 9814-9819

**Table 1. Color segregation quantification in the absence of CP as a function of VASP variants in the polymerization mix.**

| VASP form added (50 nM) | % segregation | Number of beads analyzed | p value |
|---|---|---|---|
| WT VASP | 95% | 93 | -- |
| ΔFAB-VASP | 23% | 69 | $p < 0.0001$[a] |
| No addition | 13% | 90 | $p < 0.0001$[a]<br>$p = 0.1$[b] (n.s.) |
| ΔGAB-VASP | 88% | 86 | $p = 0.09$[a] (n.s.) |
| ΔPP-VASP | 78% | 68 | $p = 0.0012$[a] |
| ΔEVH1-VASP | 73% | 82 | $p = 0.0001$[a] |
| ΔTET-VASP | 78% | 117 | $p = 0.0005$[a] |

Arp2/3 complex concentration is 50 nM. n.s. indicates a non-significant difference.

[a] As compared to WT VASP.

[b] As compared to ΔFAB-VASP.

**Figure legends**

**Figure 1: VASP can replace CP in bead motility and polarized actin network growth.**
A) 1 μm diameter beads form actin comets and move in the presence of 25 nM CP or without CP but with 50 nM added VASP. Reaction time is approximately 8 minutes. B) The polarity of actin assembly on 4.5 μm beads is assessed with a two-color assay in the presence or absence of 25 nM CP, and in the absence of CP with 50 nM added VASP. The first color is magenta (actin Alexa 594) and the second is green (actin Alexa 488). Separate channels and overlay images are shown (colocalization is white in the magenta/green overlays). Linescans are taken as indicated by white lines, and fluorescence intensity (arbitrary units) is plotted versus distance from the bead center. Superposition of magenta and green curves indicates unpolarized growth, and separation of magenta and green curves indicates polarized growth. For all panels, the concentration of the Arp2/3 complex is 50 nM. Phase contrast and epifluorescence microscopy. All scale bars 5 μm.

**Figure 2: Interplay of Arp2/3 complex activity and VASP for polarized actin growth in the absence of CP.** The extent of polarized actin growth on 4.5 μm beads is assessed using the two-color approach. A) Separate channels and overlay images are shown (first color magenta, representing actin Alexa 594, second color green, representing actin Alexa 488). Linescans are measured as indicated by white lines, fluorescence intensity (arbitrary units) is plotted versus distance from the bead center, and separation of magenta and green curve maxima is taken as a segregation event, indicative of polarized growth. Top panels: actin growth in the presence of excess (150 nM) Arp2/3 complex in the absence of CP and VASP. Bottom panels: beads are coated with a tetrameric form of pVCA (Streptavidin-pVCA or S-pVCA), which is a more effective activator of the Arp2/3 complex than GST-pVCA. The polymerization mix contains no CP and no VASP, and 50 nM Arp2/3 complex. B) Actin growth in the presence of varying amounts of the Arp2/3 complex and VASP in the absence of CP. Overlay images are shown. % color segregation and number of beads analyzed is indicated on an image of each condition; images were chosen to represent the majority case for each condition. The phase space where segregation occurs more than 50% of the time is depicted by the red boundary. C) Images of actin and Arp2/3 complex in 25 nM CP and no CP/37 nM VASP conditions at about 10 minutes reaction time. The Arp2/3 complex concentration is 50 nM. A medial plane is shown. Quantification of total fluorescent intensity in the actin and Arp2/3 complex channels. $N \geq 7$. n.s. indicates a non-significant difference. A) and B) epifluorescence microscopy. C) spinning disc microscopy. All scale bars 5 μm.

**Figure 3: How the actin network grows with other elongators and over time.**
A) Separate channels and overlay images are shown (first color magenta, representing actin Alexa 594, second color green, representing actin Alexa 488). Linescans are measured as indicated by white lines, fluorescence intensity (arbitrary units) is plotted versus distance from the bead center, and separation of magenta and green curve maxima is taken as a segregation event, indicative of polarized growth. Top panels: actin growth in the presence of 100 nM chimeric human/*Dictyostelium* VASP dimer (VASP-2M). Color segregation occurs on 80% of the beads (N = 88). Bottom panels: actin growth in the presence of 50 nM FMNL2-8P, which gave 0% color segregation (N = 44). Epifluorescence microscopy. Scale bar 5 μm. B) Evolution over time of the total fluorescence of the actin network (medial plane, spinning disc images) in no CP/37 nM VASP conditions (open symbols) and in 25 nM CP conditions (closed symbols). Linear fits are shown. The Arp2/3 complex concentration is 50 nM. $N \geq 8$ beads for each condition. S.D. are large because of low signal to noise in spinning disc slices, but differences between no CP/+VASP and +CP conditions are significant except for actin fluorescence at 1 minute.

**Figure 1 Abou-Ghali et al.**

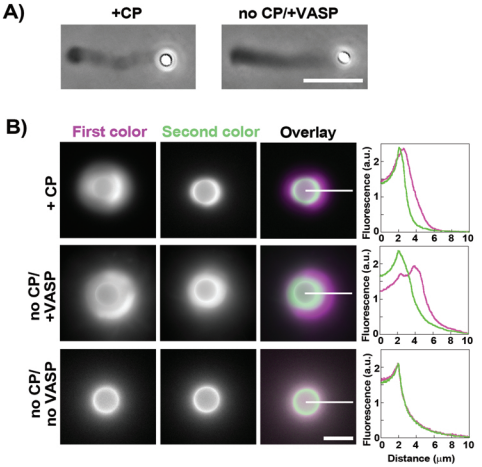

**Figure 2 Abou-Ghali et al.**

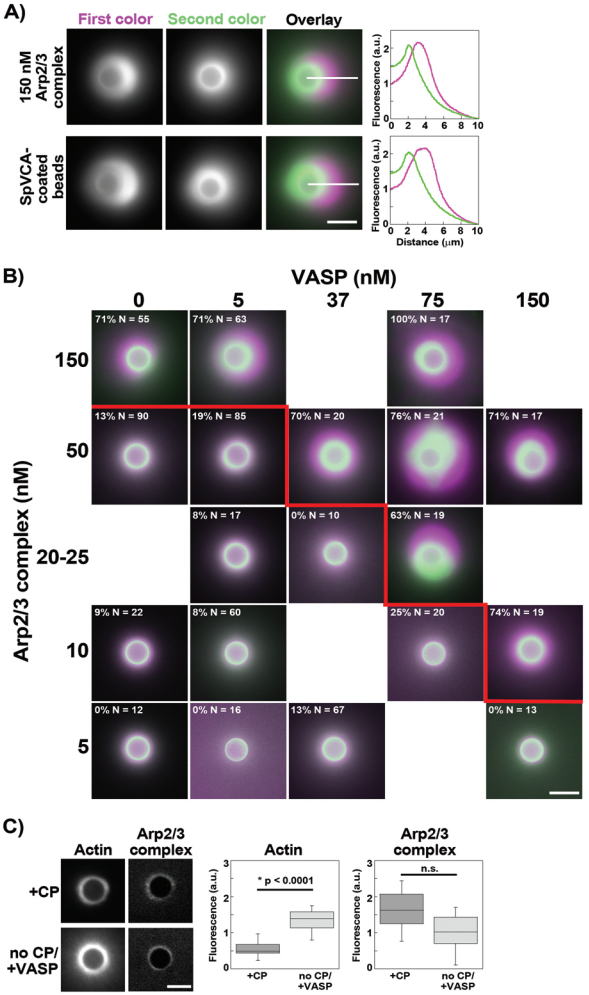

**Figure 3 Abou-Ghali et al.**